Dual-Isotope SPECT Using Simultaneous Acquisition of ^{99m}Tc and ^{123}I Radioisotopes: A Double-Injection Technique for Peri-Ictal Functional Neuroimaging

Benjamin H. Brinkmann, Michael K. O'Connor, Terence J. O'Brien, Brian P. Mullan, Elson L. So and Richard A. Robb

Biomedical Imaging Resource, Departments of Nuclear Medicine and Neurology, Mayo Clinic, Rochester, Minnesota; Australian Center for Clinical Neuropharmacology and Department of Clinical Neurosciences, St. Vincent's Hospital, Melbourne, Australia

The acquisition of multiple radiotracer studies at different time points during a neurological event permits the study of different functional activation states in humans. Peri-ictal SPECT is a promising technique for localizing the epileptogenic zone and would be enhanced by the ability to acquire sequentially coregistered ictal and postictal SPECT images of a single seizure. This study was designed to develop and validate an accurate method for the simultaneous acquisition of ^{99m}Tc and ^{123}I SPECT images of the brain. **Methods:** A multicompartment, transaxial Hoffman brain-slice phantom was filled with ^{99m}Tc, ^{123}I or a 3:1 mixture of the two isotopes. Planar and SPECT images were acquired by a dual-head gamma camera system equipped with parallel and fanbeam collimators, respectively. Thirty-two energy windows (2 keV width) were acquired over the energy range 120–184 keV. From the planar data, the signal-to-noise characteristics and crosstalk were measured for each energy window and used to devise an energy window acquisition strategy that was then applied to the SPECT data. Three summed energy windows were created: a primary ^{99m}Tc image (130–146 keV), a primary ^{123}I image (152–168 keV) and a secondary ^{99m}Tc crosstalk image (134–140 keV). A fraction (0.041) of the ^{99m}Tc crosstalk image was subtracted from the ^{123}I image. No crosstalk correction was performed on the primary ^{99m}Tc image. **Results:** (a) Planar images: results showed 1.3% crosstalk in the ^{123}I image compared with 19.7% for a 10% asymmetric energy window alone. ^{123}I crosstalk into the ^{99m}Tc window was 2.79% and was relatively constant with changes in the location of the ^{99m}Tc energy window. (b) Tomographic images: results showed 1.51% ^{99m}Tc crosstalk in the ^{123}I image compared with 12.44% for the uncorrected image and 3.70% ^{123}I crosstalk in the ^{99m}Tc image. **Conclusion:** An effective technique for the simultaneous acquisition of ^{99m}Tc and ^{123}I radiotracer distributions in the brain has been developed and validated in a phantom model and should have clinical application in peri-ictal functional activation studies of the brain.

Key Words: dual isotope; functional activation; partial epilepsy; neurological SPECT

J Nucl Med 1999; 40:677–684

Received Mar. 24, 1998; revision accepted Sep.18, 1998.

For correspondence or reprints contact: Michael K. O'Connor, PhD, Section of Nuclear Medicine, Charlton 1-225, Mayo Clinic, Rochester, MN 55905.

Peri-ictal SPECT is a potentially powerful tool to study changes in regional cerebral blood flow (rCBF) during and after a partial seizure, as well as to aid in the localization of the seizure focus during the presurgical evaluation of patients with intractable partial epilepsy. Peri-ictal SPECT involves intravenous injection of a radiotracer with a high first-pass cerebral extraction rate and low backdiffusion, such as ^{99m}Tc-hexamethyl propyleneamine oxime (HMPAO), ^{99m}Tc-ethyl cysteinate dimer (ECD) or ^{123}I-iodoamphetamine (IMP), during (ictal SPECT) or immediately after (postictal SPECT) a partial seizure. The peri-ictal SPECT images then can be acquired up to several hours later, providing a semiquantitative image of the rCBF pattern present approximately 30–120 s after the injection (*1,2*). In an attempt to improve the utility of peri-ictal SPECT, we have developed and validated a method known as subtraction ictal SPECT coregistered to MRI (SISCOM). This method coregisters and normalizes the interictal SPECT to the ictal SPECT and then derives a difference image coregistered to the patient's MR image (*3*). In a subsequent blinded study, it was shown that SISCOM significantly improves clinical outcomes in surgery patients (*4*). Other groups have independently reported methods for creating subtraction (or "difference") SPECT images co-registered to MRI and also found that these methods improve sensitivity and specificity compared with unaided visual SPECT analysis (*5–8*). In addition, we performed a pilot study that suggested that the SISCOM method may have a role in cerebral activation studies (*9*).

One of the continuing limitations of using peri-ictal SPECT as a tool for studying seizures is that, whereas seizures are a dynamic phenomenon, SPECT is able to give only a single "snapshot" of the blood-flow pattern during the limited time window of a seizure. It is therefore very difficult, with current SPECT methods, to study the evolution of blood-flow changes occurring during and after an epileptic seizure. Partial seizures have long been known to be associated with a transient focal increase in cerebral

blood flow in the region of the seizure focus (*10–13*), but more recently it has been found that many patients will also show prominent focal hypoperfusion at the epileptogenic zone postictally (*1,2,8,14–18*). A dual-isotope, double-injection technique using sequential injections of two radiopharmaceuticals with different photopeaks, for example, ^{99m}Tc-ECD or ^{99m}Tc-HMPAO followed by ^{123}I-IMP, to produce two different simultaneously acquired images has great potential as a tool for studying peri-ictal blood flow by documenting the changes occurring over time during a single seizure. Because both ^{99m}Tc-ECD (*19,20*) and ^{123}I-IMP (*21–24*) show similar brain uptake kinetics that closely reflect the pattern of cerebral blood flow shortly after their injection, the differences between the images should reflect the changes in the cerebral blood flow pattern that occur between the injections.

The dual-isotope, double-injection method has great potential to further improve the sensitivity and specificity of SISCOM in localizing partial epilepsy by allowing the subtraction of a postictal image from a simultaneously acquired ictal image. The traditional SISCOM technique has required that the ictal and interictal SPECT images, which are acquired at different times, be coregistered to one another before quantitative analysis. One of the major determinants of the signal-to-noise ratio in the subtraction image (and therefore its sensitivity and specificity) is the accuracy of this SPECT-to-SPECT coregistration. Our current method of coregistration has produced a matching accuracy of better than 1 voxel dimension (*3*). Although registration algorithms have improved in automation and accuracy in recent years, most algorithms require user interaction, and no algorithm, to our knowledge, is more accurate than a half voxel (*25*). Misalignments of this magnitude have been shown to result in significant errors in blood-flow estimates (*26*). With the dual-isotope, double-injection technique, the ictal and postictal images will be acquired at the same time and, therefore, will be perfectly coregistered, removing this source of measurement error entirely. In addition, the magnitude of the focal hypoperfusion in postictal SPECT is generally greater and more reliable than that in interictal SPECT (*15–18*). As a result, the magnitude of the focal difference in the subtraction images in the region of the epileptogenic zone should be greater by subtracting a postictal SPECT, rather than an interictal SPECT, from the ictal SPECT. An additional advantage of this technique is that it avoids the inconvenience and expense to the patient of having to return to the institution for a separate interictal SPECT.

The essential prerequisite to the development of a clinically useful double-injection, dual-isotope technique for brain studies is to be able to acquire simultaneously two separate ^{99m}Tc and ^{123}I images with minimal crosstalk and spatial resolution comparable to current single-isotope ^{99m}Tc images. The purpose of this article is to report and validate an original method, suitable for routine clinical use, for simultaneously acquiring two separate tomographic SPECT images of ^{99m}Tc and ^{123}I uptake in the brain.

MATERIALS AND METHODS

Brain-Slice Phantom

A two-dimensional brain-slice phantom (Hoffman phantom; Data Spectrum Corp., Chapel Hill, NC) was used. This phantom consisted of seven independent compartments, simulating realistic uptake of cerebral blood-flow agents in the cortex and white matter areas of the brain. The phantom represents a two-dimensional transaxial slice through the lentiform nucleus and corpus callosum. As shown in Figure 1, compartments 1–4 (total volume 18.6 mL) in the anterior left section of the phantom were designated ^{123}I-only compartments, whereas compartments 5 and 6 (total volume 12.3 mL) in the posterior left section of the phantom were designated ^{99m}Tc-only compartments. Compartment 7 (96.3 mL) was designated for mixed isotopes. The phantom's perimeter was covered by a layer of simulated bone to replicate bone scatter in tomographic acquisitions.

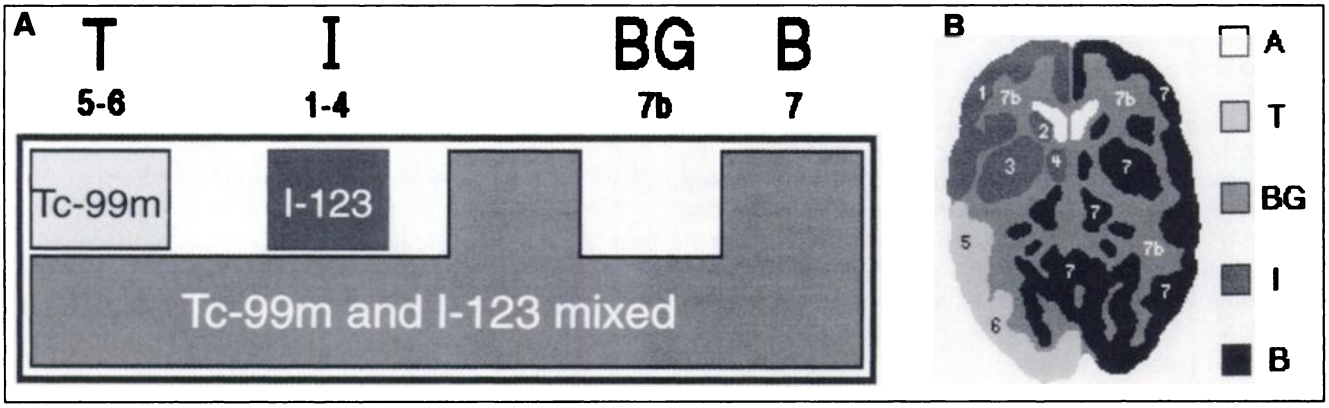

FIGURE 1. (A) Simulated cross section through two-dimensional Hoffman brain-slice phantom. Gray matter is simulated by areas where isotopes are present in both layers of phantom, and white matter (cerebral background) is simulated by areas with isotopes in bottom layer only. Labels correspond to areas shown in (B), and numbers correspond to phantom's compartments. (B) Planar representation of two-dimensional Hoffman brain-slice phantom. Areas are both isotopes (B), ^{123}I area (I), both isotopes in bottom layer only (BG), ^{99m}Tc area (T) and isotope-free areas (A). Numbers identify various isotope compartments in phantom.

Planar Images

Energy Channel Analysis. Planar images of the brain phantom were acquired using one head of a dual-head gamma camera system (Helix; Elscint, Inc., Haifa, Israel) equipped with a high-resolution parallel-hole collimator. Foam pads were taped to the collimator as a template for positioning the phantom. Acquisitions were performed using 32 contiguous energy channels, each 2 keV in width, from 120 to 184 keV. Data were acquired into a 256 × 256 matrix, with a zoom of 2, giving an effective pixel size of 1.1 mm. Three types of acquisitions were performed and numbered as (1) ^{123}I-only: compartments 1–4 and 7 were filled with ^{123}I, while compartments 5 and 6 were filled with water; (2) ^{99m}Tc-only: compartments 5–7 were filled with ^{99m}Tc, while compartments 1–4 were filled with water; and (3) dual isotope: compartments 1–4 were filled with ^{123}I only, compartments 5 and 6 were filled with ^{99m}Tc only and compartment 7 was filled with a ^{99m}Tc-to-^{123}I activity ratio of 3:1.

Figure 2 illustrates the dual-isotope, ^{123}I-only and ^{99m}Tc-only acquisitions. The 32 images from the dual-isotope acquisition were transferred to a Unix workstation (Silicon Graphics, Inc., Mountain View, CA). Region of interest (ROI) analysis was performed on each of the 2-keV band images using the Analyze AVW software package (Mayo Foundation, Rochester, MN) (*27*). Five different regions of each image were analyzed. These were labeled (A) a background region outside the brain, (I) a region over compartments 1–4, (T) a region over compartments 5 and 6, (B) a region over compartment 7 and (BG) a region over the "white matter" region of compartment 7. Note that a portion of compartment 7 overlaps compartments 1–4 and compartments 5 and 6. Hence, the region BG was used to remove the contribution of activity in compartment 7 from activity measured in the other compartments. The ROIs are shown in Figure 3A. The average counts per pixel from these regions were determined for the 32 energy channels and were used to calculate signal above baseline (SAB) and percent crosstalk (PC) as follows:

$$SAB_{TC} = T - BG, \qquad SAB_I = I - BG,$$

$$PC(\text{Tc to I}) = SAB_{TC}/SAB_I \times 100\%,$$

$$PC(\text{I to Tc}) = SAB_I/SAB_{TC} \times 100\%.$$

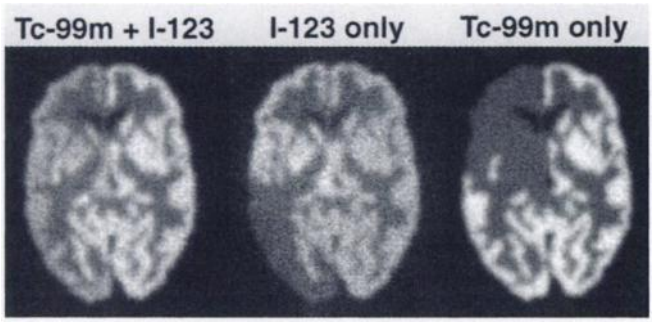

FIGURE 2. Planar images of brain-slice phantom obtained from dual-isotope (left), ^{123}I-only (center) and ^{99m}Tc-only (right) planar acquisitions. Energy windows were set to 146–162, 143–175 and 126–145 keV, respectively. (Dual-isotope window was chosen to show roughly equal amounts of ^{99m}Tc and ^{123}I activity.)

The parameter SAB represents the signal in the single-isotope compartments, and PC represents crosstalk from the opposing isotope as a percentage of each isotope's signal. These parameters were used to determine the best combination of energy window settings for the ^{99m}Tc and ^{123}I signals. A third parameter, the signal-to-noise ratio (SNR) was derived from the equation:

$$SNR = SAB/A.$$

SNR depends on the total activity in the phantom and the acquisition time and, hence, should not be used to compare between different acquisitions.

Using the Analyze AVW software, various combinations of energy channels were summed to generate composite images equivalent to images that would be acquired using an energy window spanning the included energy channels. This technique was used to test various energy window settings and to reproduce methods previously reported in the literature (to within 1 keV) for planar images. Most previous authors have used a 10% energy window centered on the ^{99m}Tc photopeak (*28–30*) and either a slightly asymmetric (153–169 or 155–171 keV) 10% ^{123}I energy window (*29,30*) or a very asymmetric 10% (159–175 keV) energy window that excludes the lower half of the photopeak (*28,31*). Our optimal energy window settings were chosen based on values for SAB, PC and SNR. The optimized crosstalk-corrected images were compared to similar images (identical energy windows) generated from the ^{99m}Tc-only (acquisition #1) and ^{123}I-only (acquisition #2) studies. In addition, our acquisition strategies were applied to ^{99m}Tc-only and ^{123}I-only datasets, and the counting statistics of these images were compared to images generated using the 20% centered energy windows commonly used in single-isotope acquisitions.

Crosstalk Compensation

Crosstalk from ^{99m}Tc represented a significant problem in the relatively count-poor ^{123}I image, particularly in the lower half of the ^{123}I photopeak. To correct for this crosstalk, a fraction of the ^{99m}Tc photopeak signal was subtracted from the ^{123}I image. A 4% asymmetric window (134–140 keV) was used to isolate the ^{99m}Tc signal from ^{123}I contamination and septal penetration. This provided a spatial map of the ^{99m}Tc crosstalk in the ^{123}I window. The contamination correction fraction was calculated from acquisition #2 (the ^{99m}Tc-only study). The counts in the ^{99m}Tc compartments were measured as a function of the energy channels. The counts in each energy channel were divided by the counts in the 4% photopeak image to yield a correction factor. Correction factors less than 0.0005 were observed to consist primarily of background noise and were therefore set to zero. The total correction factor for a given energy window was obtained by summing the appropriate correction factors for the energy channels contained within the energy window. To verify the crosstalk correction from ^{99m}Tc into the ^{123}I energy window, we applied our optimized technique to the ^{99m}Tc-only dataset to produce ideally an image containing only noise. An additional dual-isotope study with a ^{99m}Tc-to-^{123}I activity ratio of 6:1 was also performed to assess the technique's ability to correct for high levels of crosstalk into the ^{123}I energy window.

Tomographic Images

Tomographic images of the brain phantom were acquired using both heads of the gamma camera with high-resolution fanbeam collimators. The brain phantom was taped to the headrest and its location marked to facilitate repositioning. Acquisitions were

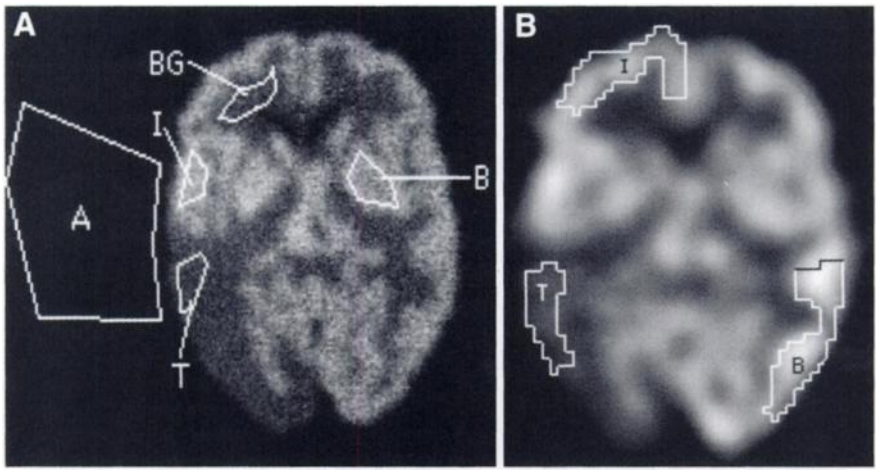

FIGURE 3. (A) Planar image of brain shows ROIs used in calculating SAB, PC and SNR. Regions are labeled as (A) background region outside brain, (I) region over compartments 1–4, (T) region over compartments 5 and 6, (B) region over compartment 7 and (BG) region over "white matter" area of compartment 7. (B) Tomographic image of brain shows ROIs used in validating accuracy of crosstalk correction technique. Labels are consistent with (A).

performed using 32 contiguous energy channels, each 2 keV in width, from 120 to 184 keV. Data were acquired into a 64 × 64 matrix, with a zoom of 1.4, giving an effective pixel size of 3.1 mm. The three types of acquisitions described above for planar studies were repeated with SPECT. Image data were reconstructed using a standard filtered-backprojection algorithm with a Metz filter (power = 3, full width at half maximum = 6 mm). The Metz filter was fixed and not count dependent.

Dual-isotope ^{99m}Tc and ^{123}I images were acquired on the basis of the analysis of the planar images. Simple energy windows from the ^{99m}Tc-only and ^{123}I-only acquisitions were used to create reference images. ROI analysis was performed to compare the crosstalk-corrected and reference images. Three different regions of each image were analyzed and labeled as (I) a region over compartments 1–4, (T) a region over compartments 5 and 6 and (B) a region over compartment 7 (Fig. 3B). Ratios of counts (T/B for the ^{123}I images and I/B for the ^{99m}Tc images) were calculated for each of the crosstalk-corrected images and compared to the corresponding ratios for the reference single-isotope images.

To determine the attenuation coefficients for use with ^{99m}Tc and ^{123}I and a low-energy fanbeam collimator, our acquisition strategy was applied to tomographic acquisitions of an anthropomorphic head phantom (Radiology Support Devices, Long Beach, CA) filled with a 3:1 mixture of ^{99m}Tc and ^{123}I. This phantom consisted of a uniform water chamber filling the cranial cavity of a simulated human skull. Attenuation correction was performed on the reconstructed transaxial slices using the method of Chang (*32*). Values of the attenuation coefficient varied between 0.0 and 0.14 cm^{-1}, and optimum values were determined by placing an ROI around activity in a 1.76-cm-thick transaxial slice of the midbrain and minimizing the coefficient of variation (SD/mean) of counts within the region. This method was applied in place of the more traditional approach of adjusting the attenuation coefficient to yield a flat count profile across the brain, since previous work has shown this method to be unreliable. The nonuniform effects of bone attenuation alter the shape of the profile and make it impossible to determine a single value of the attenuation coefficient that will yield a flat count profile for all regions of the brain (*33*).

If there is no difference in the spatial distribution of the ^{99m}Tc and ^{123}I photopeak events, subtraction of an ^{123}I image from its corresponding ^{99m}Tc image should produce an image containing only noise and reconstruction artifact. To verify this, a tomographic acquisition was performed using our dual-isotope acquisition strategy on a three-dimensional brain phantom (three-dimensional Hoffman phantom; Data Spectrum Corp.) filled uniformly with a 3:1 mixture of ^{99m}Tc and ^{123}I. The images were reconstructed and attenuation corrected to yield the ^{99m}Tc transaxial images and the crosstalk-corrected ^{123}I transaxial images. Both image volumes were normalized to a mean cerebral pixel count of 100 and subtracted (*3*).

RESULTS

Planar Images

Figure 4 plots the SAB and the isotope-to-isotope PC for ^{99m}Tc and ^{123}I across the acquired energy spectrum. It illustrates that the ^{99m}Tc and ^{123}I signals show significant overlap and crosstalk between 145 and 155 keV. As a result of the abundance of ^{99m}Tc counts below 146 keV, a clean ^{99m}Tc image with minimal crosstalk and a good SNR can be constructed by simply restricting the energy window to below this level. Therefore, for the ^{99m}Tc image, we used a 12% (130–146 keV) asymmetric window, which maximized the ^{99m}Tc counts in the image while minimizing ^{123}I crosstalk. Figure 5 compares the dual-isotope ^{99m}Tc planar image with the reference ^{99m}Tc-only planar image. The ^{99m}Tc image contained 2.79% PC and had an SNR of 180. The previously reported (*28,30*) asymmetric 10% energy window (133–147 keV) contained 3.60% PC and had an SNR of 186. Applying our acquisition strategy to the ^{99m}Tc-only data resulted in an image with 18% fewer counts compared to an image generated using the standard single-isotope 20% energy window.

We found that the optimum ^{123}I image was obtained using an energy window of 152–168 keV (10%) with crosstalk correction. This correction was performed by subtracting 0.041 of the ^{99m}Tc crosstalk image (134–140 keV) from the ^{123}I image. The 152–168 keV energy window without

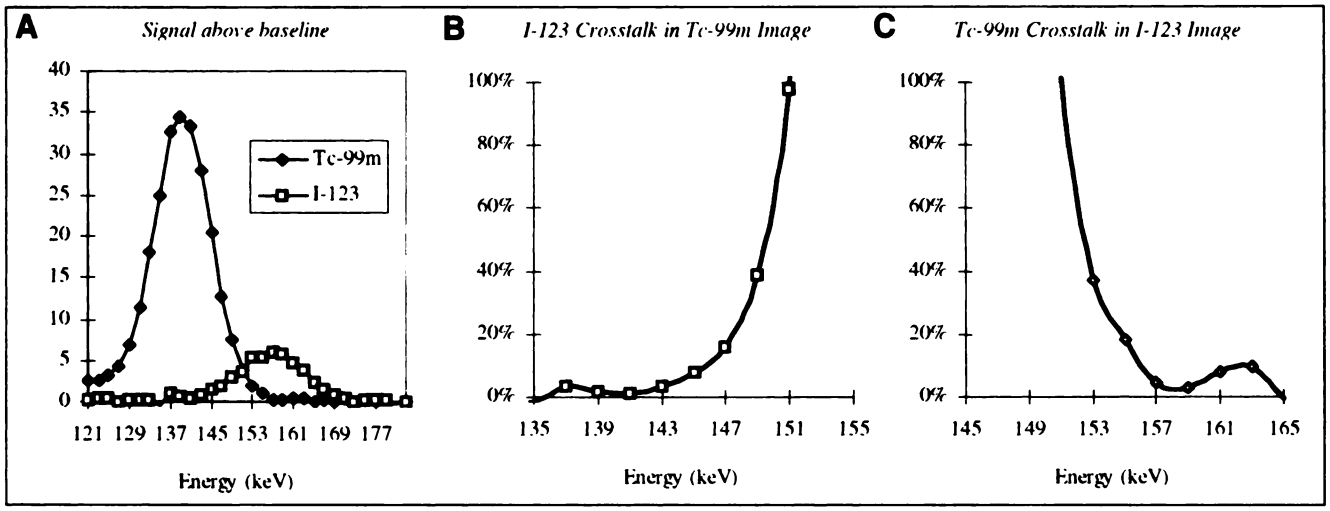

FIGURE 4. (A) Signal above baseline (SAB) plotted as function of energy for ^{99m}Tc and ^{123}I. (B) Percent crosstalk from ^{123}I into ^{99m}Tc for each energy channel [PC(I to Tc)]. ^{123}I contamination of ^{99m}Tc data is less than 10% below 145 keV. (C) Percent crosstalk from ^{99m}Tc into ^{123}I for each energy channel [PC(Tc to I)]. ^{99m}Tc contamination of ^{123}I data becomes significant (> 40%) below 153 keV.

crosstalk correction (nearly identical to a previously reported method [*29*]) produced 19.7% crosstalk into the ^{123}I image from ^{99m}Tc. Applying crosstalk correction reduced the ^{99m}Tc crosstalk to 1.33% but decreased the SNR from 16.3 to 14.7. Shifting the ^{123}I energy window up to 159–175 keV (*28,31*) resulted in only 3.65% crosstalk; however, this reduced the SNR by a factor of 2, to 7.98. The planar dual-isotope ^{99m}Tc and ^{123}I images are shown compared to their reference counterparts in Figures 5 and 6, respectively. Applying the crosstalk correction method to the ^{99m}Tc-only acquisition resulted in an image containing only noise. When the optimized ^{123}I crosstalk-corrected strategy was applied to the ^{123}I-only acquisition, there was a 48% reduction in counts compared to those obtained with a standard 20% energy window. However, the 153–169 keV technique of Mathews et al. (*29*) yielded a 37% reduction in counts, and the 159–175 keV window method of Ivanovic et al. (*28*) and Devous et al. (*31*) resulted in a 58% reduction in counts relative to a standard 20% energy window. Increasing the ^{99m}Tc-to-^{123}I ratio to 6:1 increased the ^{99m}Tc crosstalk to 28.1%, and crosstalk correction only reduced this to 7.9%.

Tomographic Images

Crosstalk correction for the ^{123}I image was applied before and after image reconstruction with essentially identical results. Post-reconstruction crosstalk correction is preferred for its practical ease and lower computation time. The tomographic dual-isotope ^{99m}Tc and ^{123}I images are shown compared to their respective reference images in Figures 7 and 8, respectively. The reference ^{123}I image had a T/B ratio of 0.3155, whereas the crosstalk-corrected dual-isotope image had a T/B ratio of 0.3202, a difference of 1.51%. A dual-isotope ^{123}I image using a 10% energy window (152–168 keV) and no crosstalk correction had a T/B ratio of 0.3547, a difference of 12.44% from the reference ^{123}I image. The dual-isotope ^{99m}Tc image had an I/B ratio of 0.2657, compared to the reference ^{99m}Tc image I/B ratio of 0.2759, a difference of 3.70%.

An attenuation correction factor of 0.04 cm^{-1} was used for the ^{99m}Tc image, and no attenuation correction was applied to the ^{123}I image. Figure 9 shows three representative transaxial images (^{99m}Tc image − normalized crosstalk-

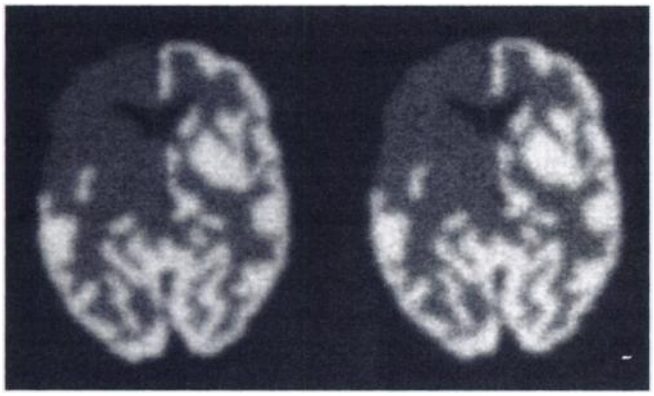

FIGURE 5. ^{99m}Tc planar dual-isotope image (left) and ^{99m}Tc planar reference image acquired without ^{123}I in phantom (right).

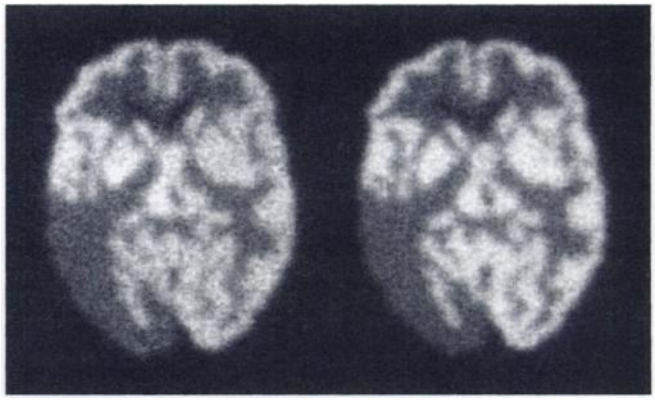

FIGURE 6. Dual-isotope ^{123}I planar crosstalk-corrected image (left) and ^{123}I planar reference image acquired without ^{99m}Tc in phantom (right).

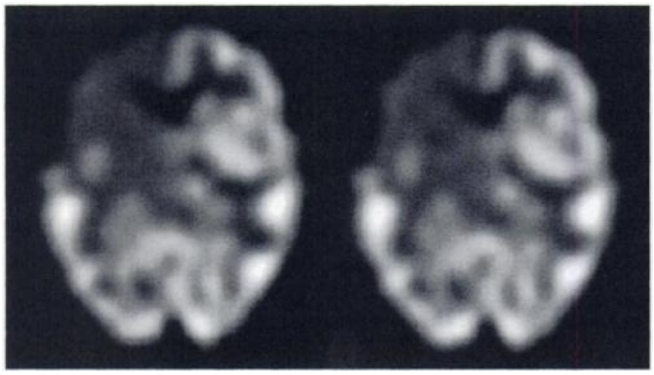

FIGURE 7. ^{99m}Tc tomographic dual-isotope image (left) and ^{99m}Tc tomographic reference image acquired without ^{123}I in phantom (right).

corrected ^{123}I image) from the three-dimensional brain phantom. These images contain only noise and reconstruction artifacts, suggesting that the SISCOM method can be applied successfully to dual-isotope images acquired with the reported strategy.

DISCUSSION

In this article we have described a method for simultaneously acquiring separate high-resolution images of ^{99m}Tc- and ^{123}I-radiolabeled tracers. The technique was developed and validated using a two-dimensional phantom and planar techniques. However, we have shown that this method is effective for tomographic imaging of three-dimensional objects and that interslice scatter and crosstalk, which are not present in the case of a two-dimensional phantom, do not confound the technique (Figs. 7–9). Although few gamma camera systems permit image acquisition with 32 energy channels, the technique described in this study requires only the ability to acquire the three energy windows defined for ^{99m}Tc, ^{123}I and ^{99m}Tc crosstalk. Our experience also suggests that the technique remains successful with minor changes to the ^{99m}Tc crosstalk-correction energy window, although a new crosstalk-correction fraction must then be calculated.

Using phantom studies we have shown that our method

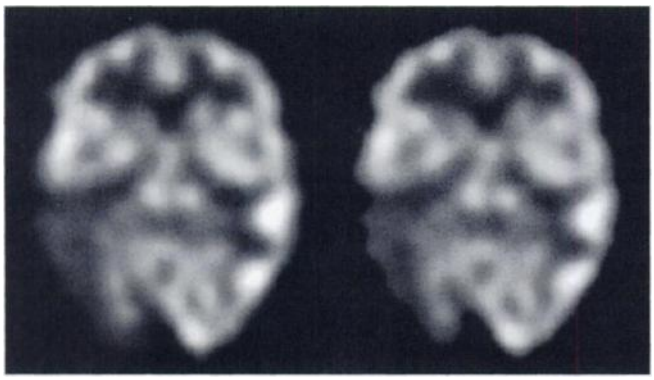

FIGURE 8. Dual-isotope ^{123}I tomographic crosstalk-corrected image (left) and ^{123}I tomographic reference image acquired without ^{99m}Tc present in phantom (right).

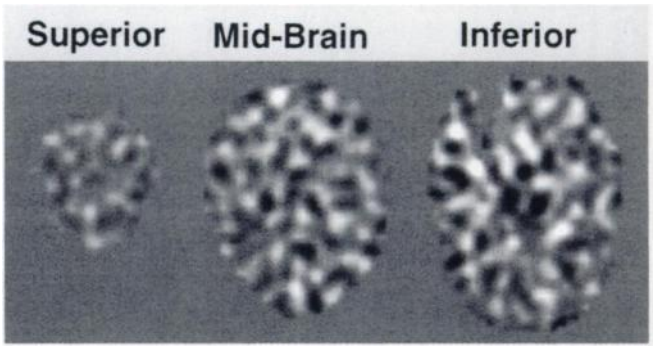

FIGURE 9. Subtraction images (^{99m}Tc image − normalized crosstalk-corrected ^{123}I image) from reconstructed transaxial slices through three-dimensional Hoffman brain phantom. Phantom contained 3:1 mixture of ^{99m}Tc and ^{123}I. Representative slices are shown from superior, central and inferior sections of brain phantom and show only noise.

can produce two clinically usable images with minimal isotope crosstalk and satisfactory SNR for both planar and tomographic acquisitions. No previous work to our knowledge has used a pixel-by-pixel analysis of the isotopes' energy spectra to devise and validate an acquisition strategy. Narrowing the acquisition window to 10% and applying subtractive crosstalk correction for the ^{123}I image does reduce total image counts substantially, relative to a standard single-isotope 20% symmetric energy window, but some loss is necessary in a dual-isotope acquisition to separate the two isotope signals. Subtractive crosstalk correction is important for the dual-isotope method to produce satisfactory ^{123}I images, because it allows acquisition of a greater portion of the lower half of the ^{123}I photopeak without ^{99m}Tc crosstalk contamination. Most previous studies have ignored this crosstalk component (*29,30*) and have used simple energy windows with no crosstalk correction. This is unacceptable for our purposes, because the ^{99m}Tc crosstalk remaining in the ^{123}I image will corrupt any ictal to postictal comparisons. Other studies (*28,31*), which have shifted the energy window toward higher energies to avoid crosstalk, exclude nearly half the ^{123}I photopeak and reduce the SNR. In addition, much of this reduction in counts occurs by excluding scattered and septal penetration counts from the image, rather than photopeak events. One study has proposed solving crosstalk equations for the ^{123}I and ^{99m}Tc photopeak signals (*34*). To our knowledge, no formal validation of this method has been published, but the method was tested by a different group (*28*), who found it unsuitable because of spatial variation in the crosstalk fraction. Our results confirm that there is spatial variation in the ^{123}I crosstalk into the ^{99m}Tc window. However, we observed no spatial variation in the ^{99m}Tc crosstalk into the ^{123}I window, other than the tendency for noise to increase in the high signal areas, which we regard as a reflection of the noise characteristics of the two images. Several filter-based crosstalk-correction methods have been proposed for crosstalk correction (*35,36*). These techniques are most

useful in cases in which there is a large difference in the photopeak energies of the two isotopes.

The ^{99m}Tc image is aided by its high counting rate relative to the ^{123}I image, and the small amount of ^{123}I contamination in the ^{99m}Tc image is overwhelmed by the strong ^{99m}Tc signal. Because the ^{123}I crosstalk in the ^{99m}Tc window is dominated by spatially uncorrelated scatter and septal penetration, a subtractive crosstalk-correction method (as was used for the ^{123}I image) is not feasible unless accurate scatter correction could be applied. However, limiting the ^{99m}Tc energy window below 146 keV to remove the ^{123}I contamination kills a very small portion of the total ^{99m}Tc counts, and such methods (which are often computationally intensive) appear unnecessary. The clinical dose limits for these two radioisotopes suggest a 6:1 ^{99m}Tc-to-^{123}I ratio. However, because acquisition time is dictated by the relatively count-poor ^{123}I image, and because crosstalk correction at this high ratio is more difficult, we have elected to reduce patient dose and use a 3:1 ^{99m}Tc-to-^{123}I ratio, which does not degrade the ^{99m}Tc image significantly. Previous work by Devous et al. (*31*) has shown that downscatter from ^{123}I into the ^{99m}Tc energy window is relatively small even at a 1:1 ratio of the two isotopes.

The attenuation coefficient for ^{99m}Tc is assigned a value of 0.12 cm^{-1} in a uniform attenuating material (*37*). However, the presence of bone in the skull has been shown to decrease the optimum value for the attenuation coefficient to approximately 0.09 cm^{-1} (*33,38*). This paradoxical decrease has been shown both theoretically and experimentally to be caused by the effects of outer layers of attenuating material that are free of radioactivity (*33*). It has also been shown (*33*) that the use of a fanbeam collimator further reduces the optimum value of the attenuation coefficient (μ = 0.07 cm^{-1}). The addition of septal penetration from the high-energy emissions of ^{123}I increases the apparent activity in the center of the brain and would be expected to further reduce the optimum attenuation coefficient. This was verified in our experiments. Attenuation coefficients are likely to be affected by changes in collimator design (focal length, septal thickness, etc.), and, hence, our results may not be applicable to other fanbeam collimators.

CONCLUSION

This study has demonstrated that clinically satisfactory ^{99m}Tc and ^{123}I tomographic images with minimal isotope-to-isotope crosstalk can be acquired simultaneously using carefully chosen energy windows and by subtracting ^{99m}Tc crosstalk from the ^{123}I image. ^{99m}Tc crosstalk correction is essential in constructing the ^{123}I image, resulting in improved image quality while averting the need to exclude a large portion of the photopeak, which reduces the SNR. This method is shown to result in less than 4% crosstalk in planar and tomographic images. This method inherently provides semiquantitative maps of cerebral blood flow that are in perfect alignment with one another, removing any additional noise attributable to errors in image coregistration. This dual-isotope, double-injection technique has the potential to be a valuable research and clinical tool by providing images of cerebral blood flow at different time points during a single neurological event. It may prove especially useful in improving the localization of intractable partial epilepsy by allowing the subtraction of a postictal SPECT from a simultaneously acquired ictal SPECT. It also has the potential to distinguish between primary and secondary areas of seizure involvement by demonstrating the pathways of seizure propagation.

REFERENCES

1. Berkovic SF, Newton M, Chiron C, Dulac O. Single photon emission tomography. In: Engel J Jr, ed. *Surgical Treatment of the Epilepsies*. New York, NY: Raven Press; 1993:233–243.
2. Mullan BP, O'Connor MK, Hung J. Single photon emission computed tomography. *Neuroimaging Clin North Am.* 1995;5:647–673.
3. O'Brien TJ, O'Connor MK, Mullan BP, et al. Subtraction ictal SPECT co-registered to MRI in partial epilepsy: description and technical validation of the method with phantom and patient studies. *Nucl Med Commun.* 1998;19:31–45.
4. O'Brien TJ, So EL, Mullan BP, et al. Subtraction ictal SPECT co-registered to MRI improves clinical usefulness of SPECT in localizing the surgical seizure focus. *Neurology.* 1998;50:445–454.
5. Zubal IG, Spencer SS, Imam K, Smith EO, Wisniewski G, Hoffer PB. Difference images calculated from ictal and interictal technetium-99m-HMPAO SPECT scans of epilepsy. *J Nucl Med.* 1995;36:684–689.
6. Weder B, Oettli R, Maguire RP, Vonesch T. Partial epileptic seizure with versive movements examined by [^{99m}Tc]HM-PAO brain single photon emission computed tomography: an early postictal case study analyzed by computerized brain atlas methods. *Epilepsia.* 1996;37:68–75.
7. Chiron C, Jaminska A, Cieuta C, Vera P, Plouin P, Dulac O. Ictal and interictal subtraction ECD-SPECT in refractory childhood epilepsy. *Epilepsia.* 1997;38:9.
8. Zubal G, Spanaki-Varelas M, MacMullan J, Spencer SS. Quantitative evaluation of postictal SPECT for seizure localization [abstract]. *Epilepsia.* 1997;38:52.
9. Bouras EP, O'Brien TJ, O'Connor MK, Mullan BP, Camilleri M. A pilot study of cerebral topographic representation of rectal stimulation using ^{99m}Tc-ECD single photon emission computed tomography (SPECT) [abstract]. *Gastroenterology.* 1997;112:A703.
10. Horsley V. An address on the origin and seat of epileptic disturbance. *Br Med J.* 1892;1:693–696.
11. Penfield W, Von Santha K, Cipriani A. Cerebral blood flow during induced epileptiform seizures in animal and man. *J Neurophysiol.* 1939;2:257–267.
12. Hougaard K, Oikara T, Sveinsdottir E, Skinhog E, Ingvar D, Lassen N. Regional cerebral blood flow in focal cortical epilepsy. *Arch Neurol.* 1976;33:527–535.
13. Dymond AM, Crandall P. Oxygen availability and blood flow in the temporal lobes during spontaneous epileptic seizures in man. *Brain Res.* 1976;102:191–196.
14. Newton MR, Berkovic S. Interictal, ictal, and postictal single-photon emission computed tomography. In: Cascino G, Jack C, eds. *Neuroimaging in Epilepsy: Principles and Practice*. Boston, MA: Butterworth-Heinemann; 1997:177–192.
15. Newton MR, Berkovic SF, Austin MC, Rowe CC, McKay WJ, Bladin PF. Postictal switch in blood flow distribution and temporal lobe seizures. *J Neurol Neurosurg Psychiatry.* 1992;55:891–894.
16. Newton MR, Berkovic S, Austin M, Rowe C, McKay W, Bladin P. Ictal, postictal and interictal single-photon emission tomography in the lateralization of temporal lobe epilepsy. *Eur J Nucl Med.* 1994;21:1067–1071.
17. Rowe CC, Berkovic SF, Austin MC, McKay WJ, Bladin PF. Patterns of postictal cerebral blood flow in temporal lobe epilepsy: qualitative and quantitative analysis. *Neurology.* 1991;41:1096–1103.
18. Rowe CC, Berkovic SF, Sia STB, et al. Localization of epileptic foci with postictal single photon emission computed tomography. *Ann Neurol.* 1989;26:660–668.
19. Greenberg JH, Araki N, Karp A, et al. Quantitative measurement of regional cerebral blood flow in focal cerebral ischemia using Tc-99m-ECD [abstract]. *J Nucl Med.* 1991; 32:1070.
20. Devous MD, Payne JK, Lowe JL, Leroy RF. Comparisons of ^{99m}Tc-ECD to ^{133}Xe SPECT in normal controls and in patients with mild-moderate regional cerebral blood flow abnormalities. *J Nucl Med.* 1993;34:754–761.
21. Kuhl D, Barrco J, Huang S, et al. Quantifying local cerebral blood flow with N-isopropyl-p-I-123 iodoamphetamine (IMP) tomography. *J Nucl Med.* 1982;23: 196–203.

22. Takeshita G, Maeda H, Nakane K, et al. Quantitative measurement of regional perfusion using N-isopropyl-(iodine-123)p-iodoamphetamine and single photon emission computed tomography. *J Nucl Med.* 1992;33:1741–1749.
23. Greenberg JH, Kushner M, Rangi M, et al. Validation studies of iodine-123 iodoamphetamine as a cerebral blood flow tracer using emission tomography. *J Nucl Med.* 1990;31:1364–1369.
24. Matsuda H, Seki H, Sumiya H, et al. Quantifying local cerebral blood flow by N-isopropyl-(iodine-123)p-iodoamphetamine and single photon emission computed tomography with rotating gamma camera. *Am J Physiol Imaging.* 1986;1: 186–194.
25. West J, Fitzpatrick JM, Wang MY, et al. Comparison and evaluation of retrospective intermodality brain image registration techniques. *J Comput Assist Tomogr.* 1997;21:554–566.
26. Sychra JJ, Pavel DG, Chen Y, Jani A. The accuracy of SPECT brain activation images: propagation of registration errors. *Med Phys.* 1994;21:1927–1932.
27. Hanson DP, Robb RA, Aharon S, et al. New software toolkits for comprehensive visualization and analysis of three-dimensional multimodal biomedical images. *J Digit Imaging.* 1997;10:31–35.
28. Ivanovic M, Weber DA, Loncaric S, Franceschi D. Feasibility of dual radionuclide brain imaging with I-123 and Tc-99m. *Med Phys.* 1994;21:667–674.
29. Mathews D, Walker BS, Allen BC, Batjer H, Purdy PD. Diagnostic applications of simultaneously acquired dual-isotope single-photon emission CT scans. *Am J Neuroradiol.* 1994;15:63–71.
30. Madsen MT, O'Leary DS, Andreasen NC, Kirchner PT. Dual isotope brain SPECT imaging for monitoring cognitive activation: physical considerations. *Nucl Med Commun.* 1993;14:391–396.
31. Devous MD Sr, Lowe JL, Payne JK. Dual-isotope brain SPECT imaging with technetium and iodine-123: validation by phantom studies. *J Nucl Med.* 1992;33: 2030–2035.
32. Chang LT. A method for attenuation correction in radionuclide computed tomography. *IEEE Trans Nucl Sci.* 1978;25:638–642.
33. Stodilka RZ, Kemp BJ, Prato FS, Nicholson RL. The importance of bone attenuation in brain SPECT quantification. *J Nucl Med.* 1998;39:190–197.
34. Juni JE, Bernstein RC, Ponto RA, Nuechterlein PM. Simultaneous dual-tracer brain SPECT with Tc99m-HMPAO and I-123-iodoamphetamine: method and validation [abstract]. *J Nucl Med.* 1991;32:956–957.
35. Knesaurek K. A new dual-isotope convolution cross-talk correction method: a Tl-201/Tc-99m SPECT cardiac phantom study. *Med Phys.* 1994;21:1577–1583.
36. Links JM, Prince JL, Gupta SN. A vector Weiner filter for dual radionuclide imaging. *IEEE Trans Med Imaging.* 1996;15:700–709.
37. Harris CC, Greer KL, Jaszczak RJ, Floyd CE, Fearnow EC, Coleman RE. Tc-99m attenuation coefficients in water-filled phantoms determined with a gamma camera. *Med Phys.* 1984;11:681–685.
38. Nicholson RL, Doherty M, Wilkins K, Prato FS. Paradoxical effect of the skull on attenuation correction requirements for brain SPECT. *J Nucl Med.* 1988;29:1316.